

# Molecular dynamics simulation of silicon surface smoothing by low-energy argon cluster impact

Chang-Koo Kim, Alison Kubota, and Demetre J. Economou<sup>a)</sup>

*Plasma Processing Laboratory Department of Chemical Engineering, University of Houston, Houston, Texas 77204-4792*

(Received 26 July 1999; accepted for publication 16 September 1999)

The molecular dynamics simulation method was employed to study the mechanism of silicon (001) surface smoothing by impact of Ar<sub>16</sub> or Ar<sub>40</sub> clusters with energy at or below 20 eV per constituent atom. Smoothing of a pyramid on top of an otherwise “flat” silicon surface was used as a model system to elucidate the mechanism of cluster-substrate interaction. Surface smoothing is achieved by *lateral displacement* of substrate atoms during cluster impact. There exists an optimum energy of around 4–5 eV per constituent atom of the cluster for efficient surface smoothing; this implies that a proper energy is required for effective lateral displacement. Cluster size also affects surface smoothing because lateral displacement depends on the nonlinear effect of *multiple collisions* in the near surface region. As anticipated, damage in the substrate increases with cluster energy. © 1999 American Institute of Physics. [S0021-8979(99)08324-3]

## I. INTRODUCTION

A variety of thin film processing technologies employ ion beams for etching, deposition, or surface modification. Examples include sputtering, reactive ion beam etching, ion beam assisted deposition, and ion implantation.<sup>1</sup> However, such conventional ion beam processes may cause problems including degradation of insulators, surface damage, and deep penetration of implanted atoms.<sup>2,3</sup> One way to alleviate these problems is to use a *cluster beam*.

A cluster is an assemblage of individual atoms with a few to several thousand constituents. A cluster can be ionized and the resulting ion accelerated to the desired energy. Because there are many atoms per cluster, an *ionized cluster beam* can have low energy per atom and high atom flux at the same time. This feature can be advantageous for achieving shallow implantation, surface smoothing, low damage surface cleaning, and thin film formation.<sup>4–8</sup> In addition, the charge per constituent atom is very low, reducing charging of insulating materials.<sup>8</sup>

Cluster beam processing is distinctly different from traditional ion beam processing. The ion-solid interaction during the impact of a single ion with a few keV energy can be described by the linear cascade theory proposed by Sigmund.<sup>9</sup> In the case of cluster ion impact, however, this theory fails because nonlinear effects come into play. When a cluster impinges on a solid target, the constituent atoms of the cluster collide with one another as well as with the target atoms. It is through these nonlinear *multiple collisions* that the cluster energy is shared among the constituent atoms and the target atoms.<sup>7,8,10</sup>

Another interesting phenomenon of cluster-solid interaction is lateral displacement, i.e., “horizontal” displacement of the target atoms due to cluster impact. This effect was also

called *lateral sputtering*.<sup>10</sup> However, for low enough cluster energies, the laterally displaced target atoms are not ejected from the target, i.e., they are not sputtered. As will become evident below, the phenomenon of lateral displacement is critical for surface smoothing. In the course of cluster impact, recoiled target atoms acquire mostly lateral momentum, helping to smooth an initially rough surface. Atomically flat surfaces are of major importance in modern thin film processing.

Several researchers have studied experimentally surface smoothing by cluster ion beams. Northby *et al.*<sup>11</sup> studied the impact of 30 keV Ar<sub>300</sub> clusters on Au films. They observed surface smoothing by scanning electron microscope (SEM) examination of impacted surfaces. Akizuki *et al.*<sup>4</sup> used atomic force microscope (AFM) measurements to study surface smoothing of Cu and Pt films impacted by 10 keV CO<sub>2</sub> clusters. They found that there was an optimum cluster size, at a given cluster energy, for which smoothing was most effective. Yamaguchi *et al.*<sup>5</sup> also studied surface roughness using AFM for CO<sub>2</sub> cluster impact on a variety of surfaces. Computer simulations have also been performed to investigate surface smoothing by cluster impact. For example, Insepov and Yamada<sup>7,12</sup> simulated the impact of Ar clusters, with 50 eV/atom, on Si surfaces.

Most reported studies on surface smoothing by cluster impact have focused on reducing surface roughness. However, it has been known that damage, extending to depths greater than the mean projected range, also occurs due to cluster impact.<sup>6</sup> Therefore, not only surface smoothing but also substrate damage have to be considered to better understand the overall effect of cluster impact. Atomic scale simulations are ideally suited for this purpose.

In this article, the molecular dynamics (MD) simulation method is used to study silicon (001) surface smoothing and substrate damage induced by the impact of Ar clusters with low energy/atom. Smoothing of a pyramid on top of an otherwise “flat” silicon surface is used as a model system to

<sup>a)</sup>Author to whom correspondence should be addressed; electronic mail: economou@uh.edu

elucidate the mechanism of cluster-substrate interaction. The system behavior is described by the value of surface roughness, the number of disordered substrate atoms, and the formation of “damage” in the substrate for various cluster sizes and energies. MD is the appropriate method for this study because the positions and momenta of projectiles and target atoms can be followed, and the effect of multiple collisions and lateral displacement ascertained.

## II. MOLECULAR DYNAMICS SIMULATION PROCEDURE

### A. Interatomic potentials

Molecular dynamics is a deterministic simulation method which follows the trajectory of individual atoms by solving Newton’s equation of motion,

$$m \frac{d\mathbf{v}}{dt} = \mathbf{F}, \quad (1)$$

$$\mathbf{F} = -\nabla \phi \quad (2)$$

for each atom in the system.  $\mathbf{F}$  is the force experienced by an atom, and  $m$  and  $\mathbf{v}$  are the mass and velocity of that atom. The force is calculated as the spatial gradient of the potential field,  $\phi$ . In this study, the Stillinger–Weber (SW) potential, which consists of two-body and three-body contributions, was used for Si–Si interactions.<sup>13</sup> It is known that this potential describes the properties of crystalline silicon fairly well and stabilizes the  $(2 \times 1)$  reconstruction on the Si(001) surface.<sup>14,15</sup> Following Kubota *et al.*,<sup>15</sup> the Molière potential was used for Si–Ar interactions with an effective screening length of 0.8853 times the Firsov value. The Lennard-Jones (LJ) potential was chosen to describe Ar–Ar interactions with  $\sigma = 3.405 \text{ \AA}$  and  $\epsilon = 0.0104 \text{ eV}$ .<sup>16</sup> This potential has been used widely to study melting and evaporation of Ar clusters,<sup>16,17</sup> and cluster–cluster collision dynamics.<sup>18</sup>

### B. Target and cluster preparation and simulation procedures

A pyramid-like structure was built on top of an otherwise “flat” Si(001)  $(2 \times 1)$  reconstructed surface to serve as model roughness. The final cell consisted of 13 layers, with 338 atoms per layer, and four more layers on top forming the pyramid consisting of 43 atoms. There was a total of 4437 atoms in the cell. The bottom two layers were fixed in space. This cell was equilibrated at 300 K for 4 ps, and was used as the initial condition for cluster impacts. Figure 1 (a) shows top and (b) side views of the computational cell. The width of the base of the pyramid is less than 1/3 of the width of the cell in both lateral ( $x$  and  $y$ ) directions to minimize edge effects. Figure 1(a) shows that, excluding the pyramid, the silicon surface atoms maintain the  $(2 \times 1)$  reconstruction. Periodic boundary conditions were applied to the cell in the lateral directions. The Berendsen<sup>19</sup> heat removal method was used with a coupling constant of 10 fs. The velocity-Verlet scheme<sup>15,20</sup> was employed to obtain the positions and velocities of all atoms in the computational cell.

Ar clusters with either 16 or 40 atoms were prepared starting with an fcc lattice<sup>21</sup> with a lattice constant of 5.256

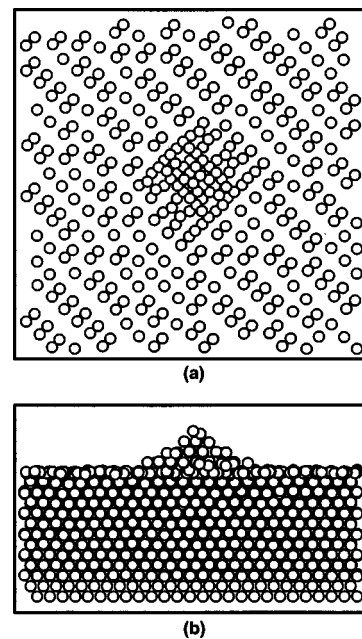


FIG. 1. (a) Top view and (b) side view of a Si(001)  $(2 \times 1)$  surface with a pyramidal protrusion on top used as the target.

$\text{\AA}$ , and removing corner atoms to obtain the desired cluster size. The resulting cluster was equilibrated at 50 K for 4 ps. The structures were very stable and maintained their total energy to seven significant figures for relatively long periods of time (10 ps). Figure 2 shows the (a)  $\text{Ar}_{16}$  and (b)  $\text{Ar}_{40}$  clusters used in this work.

The initial kinetic energy of  $\text{Ar}_{16}$  clusters was selected to be 1, 5, 10, or 20 eV/atom. The initial kinetic energy of  $\text{Ar}_{40}$  clusters was either 4 or 10 eV/atom. The cluster velocity was perpendicular to the base of the computational cell. Clusters were emitted from a distance of 4  $\text{\AA}$  above the pyramid apex. The computational cell shown in Fig. 1 was subjected to a series of impacts, each with a cluster having a specific energy and number of constituent atoms. Each of these impacts lasted 2 ps. It was verified that no significant change in the surface roughness occurred beyond 2 ps. The final lattice after a cluster impact was used as the initial condition lattice for the next impact. The effect of cluster size and energy on surface roughness and substrate damage evolution was thus studied.

## III. RESULTS AND DISCUSSION

It is instructive to follow the events during the impact of an individual cluster; this sheds light on the mechanism of cluster–solid interaction. The events described below are not

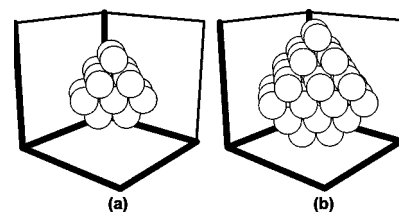


FIG. 2. Representation of (a)  $\text{Ar}_{16}$  and (b)  $\text{Ar}_{40}$  clusters.

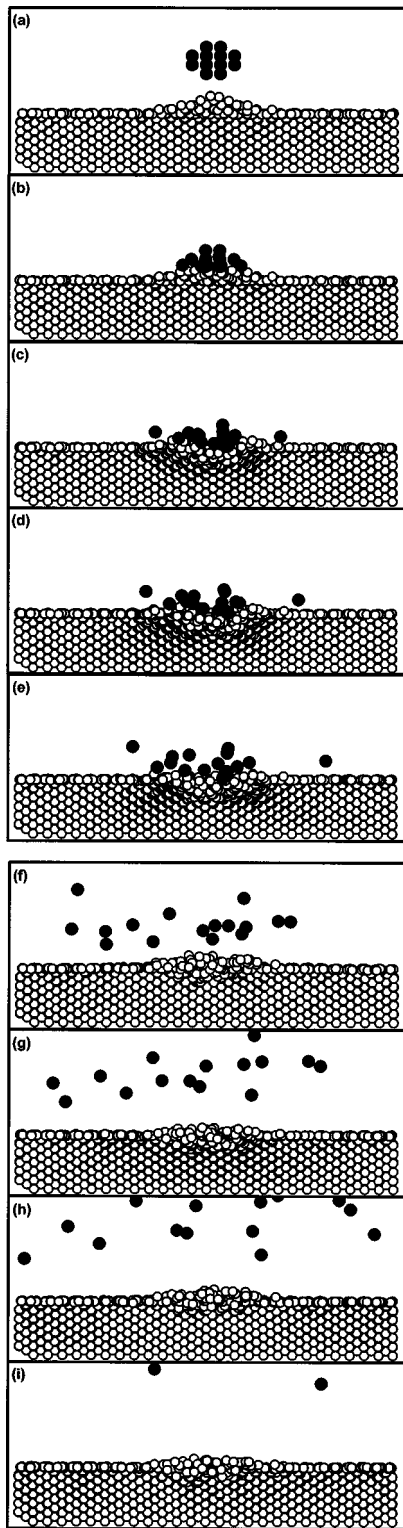


FIG. 3. Sequence of events as an  $\text{Ar}_{16}$  cluster with 10 eV/atom impinges on the surface of the cell shown in Fig. 1. Filled circles and open circles represent Ar and Si atoms, respectively. (a) 0 ps, (b) 0.115 ps, (c) 0.268 ps, (d) 0.345 ps, (e) 0.460 ps, (f) 0.958 ps, (g) 1.34 ps, (h) 1.72 ps, and (i) 4.02 ps.

specific to the individual case shown. Similar features were observed for other cluster sizes and energies.

Figure 3 is for an  $\text{Ar}_{16}$  cluster with 10 eV/atom impacting the lattice of Fig. 1. Filled and open circles represent Ar

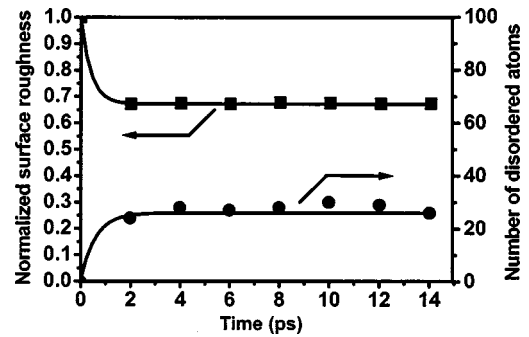


FIG. 4. Time evolution of the surface roughness and the number of disordered Si atoms for an  $\text{Ar}_{16}$  cluster with 10 eV/atom impacting the cell shown in Fig. 1.

and Si atoms, respectively. As impact begins, the cluster compresses against the silicon pyramid which in turn starts to collapse [Fig. 3(b)]. A little later, the cluster disintegrates and some Ar atoms penetrate the Si substrate slightly [Figs. 3(c), 3(d)]. Penetration would be larger for higher cluster energies. At time  $t=0.35$  ps [Fig. 3(d)], a hemispherical damaged region has formed in the substrate. The shape of this damaged region is characteristic of cluster impact, and it is very different than that due to a single ion impact. Seki *et al.*<sup>2</sup> discussed the mechanism of damage formation and suggested that the cluster energy is transferred to the substrate isotropically from the impact zone. It is interesting to note that the collapsed Si atoms are not ejected from the surface. In fact, sputtering did not occur under any of the impact cases studied. Instead, the substrate atoms are displaced laterally aiding in surface smoothing. However, the cluster-solid interaction does not end at this point.

As time elapses, Ar atoms that had previously penetrated the substrate are pushed out of the Si lattice by the Si-Ar repulsive potential [Fig. 3(e)]. Around the same time, the damaged region inside the substrate is partly repaired, but some new topography is created out of the temporarily ‘‘flattened’’ surface [compare Fig. 3(f) to 3(e)]. However, the roughness of this uneven surface is much lower than that of the pyramid on the initial surface. The surface roughness does not change significantly beyond  $\sim 2$  ps [compare Figs. 3(g) to 3(i), see also Fig. 4 below]. It is by the mechanisms of multiple collisions and lateral displacement that a rough surface is smoothed by low energy cluster impact.

The surface roughness was calculated at each time step as follows. An  $x$ - $y$  cross section of the computational cell was divided into  $(N \times M)$  subcells and the surface roughness was expressed as the variance  $R$ ,

$$R = \left( \frac{1}{NM} \sum_i^N \sum_j^M (h_{ij} - h_{av})^2 \right)^{1/2} \quad (3)$$

with

$$h_{av} = \frac{1}{NM} \sum_i^N \sum_j^M h_{ij}, \quad (4)$$

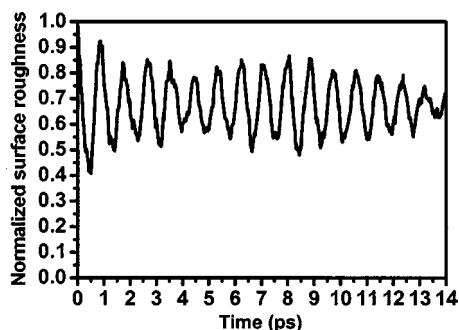


FIG. 5. Time evolution of the surface roughness for a series of impacts by  $Ar_{16}$  clusters with 10 eV/atom. Initial cell was that of Fig. 1.

where  $h_{ij}$  is the ‘‘height’’ of the  $i$ th row and  $j$ th column,  $N$  is the number of rows, and  $M$  is the number of columns of the cross section of the computational cell. The height of the  $ij$ -subcell was defined as the  $z$  coordinate of that atom in the subcell which was furthest away from an arbitrary reference plane.

Figure 4 shows the evolution of the surface roughness and the number of disordered Si atoms during the impact of an  $Ar_{16}$  cluster with 10 eV/atom on the surface of Fig. 1. Atoms displaced more than half the lattice constant from their original lattice positions are considered disordered.<sup>22</sup> The surface roughness is normalized to that of the initial Si substrate with a pyramidal protrusion on the surface (Fig. 1). Both surface roughness and the number of disordered atoms ‘‘saturate’’ after about 2 ps. Therefore, a time interval of 2 ps is enough for simulating the effects of an individual cluster impact.

Figure 5 shows the surface roughness as a function of time during serial impacts of  $Ar_{16}$  clusters with 10 eV/atom. The initial surface was that of Fig. 1. The surface roughness decreases sharply the first 0.35 ps, corresponding to the formation of the damaged region shown in Fig. 3(d). At  $t=0.5$  ps, the surface roughness starts increasing while the damage is partly repaired and surface topography is generated out of a temporarily ‘‘flattened’’ surface [Figs. 3(e) and 3(f)]. The sequence is repeated with subsequent cluster impacts. Although the surface roughness ‘‘oscillates,’’ it is always lower than the initial roughness. This cyclic behavior is characteristic of low energy cluster impact on a surface asperity. It consists of (a) initial decrease of surface roughness with subsequent formation of a damaged region, and (b) partial repair of the damaged region with subsequent increase of surface roughness. Such behavior was found to occur for all impacts simulated in this study.

Figure 6 shows the surface roughness evolution with dose for serial impacts using various Ar clusters. The surface roughness decreases and tends to saturate for Ar clusters with energy per constituent atom of 1, 4, or 5 eV. The saturation value of surface roughness depends on the energy of the constituent atoms in the cluster. The surface is smoothed most effectively for 4–5 eV/atom. The inefficiency of clusters for surface smoothing at energy/atom less than 4 eV is due to the fact that, at this low energy, lateral displacement of surface atoms is minimal. For the case of  $Ar_{40}$  clusters with 10 eV/atom, the surface roughness first decreases but

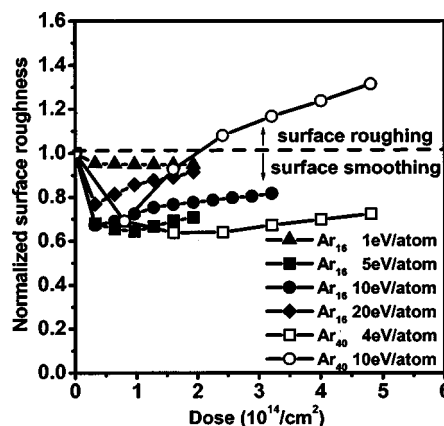


FIG. 6. Dependence of surface roughness on dose as the cell of Fig. 1 is impacted serially by Ar clusters. Each series of simulations was done with clusters of the same size and number of constituent atoms.

then increases over the initial roughness. The initial decrease of surface roughness is due to destruction of the pyramidal protrusion. However, for relatively high energies per constituent atom lateral displacement is too severe resulting, after the original protrusion has been destroyed, to higher surface roughness compared to the starting value.

The dependence of surface roughness evolution on cluster size is also seen in Fig. 6. The surface roughness after impacts by  $Ar_{16}$  clusters with 10 eV/atom is lower than that obtained with  $Ar_{40}$  clusters also having 10 eV/atom. This is due to more vigorous displacement of Si surface atoms by a larger number of multiple collisions in the case of the larger clusters.

In studying the effect of cluster impact, it is important to consider not only the surface roughness but also the degree of damage inflicted to the substrate. It is evident from Figs. 3 and 5 that, during an individual cluster impact, the surface roughness decreases while the damaged region forms, and then increases while that damaged region partly repairs itself. The degree of ultimate substrate damage after multiple cluster impacts can be estimated by the number of disordered Si atoms. Figure 7 shows the number of disordered Si atoms as a function of dose for various Ar clusters. The number of

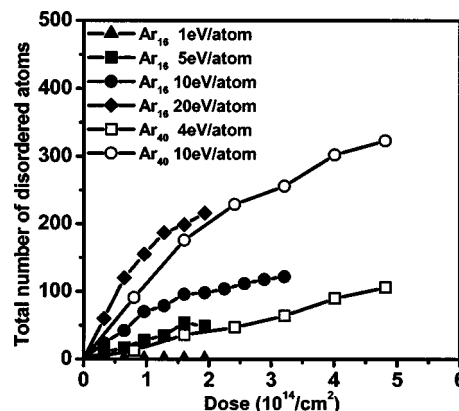


FIG. 7. Dependence of the number of disordered Si atoms on dose as the cell of Fig. 1 is impacted serially by Ar clusters. Each series of simulations was done with clusters of the same size and number of constituent atoms.

disordered atoms increases with dose. At fixed dose, the number of disordered atoms increases with the energy of constituent atoms. Thus, Ar clusters with higher energy per constituent atom induce more damage to the substrate. For the same dose, Ar<sub>16</sub> clusters with 10 eV/atom induce more damage compared to Ar<sub>40</sub> clusters with 4 eV/atom. Although both clusters have the same total energy, impact of the larger clusters (with lower energy per atom) induces relatively shallow damage; multiple collisions are confined closer to the surface. This actually promotes more efficient lateral displacement of the target atoms resulting in lower surface roughness (see Fig. 6).

#### IV. CONCLUSIONS

Surface smoothing and substrate damage due to impact of low-energy Ar clusters on Si (001) have been studied by the MD simulation method. A pyramidal protrusion on an otherwise "flat" Si surface was used as a model roughness. Cluster impact is distinctly different than single atom impact. The former is characterized by *multiple collisions* on the surface (a nonlinear effect) and *lateral displacement* of target atoms, leading to surface smoothing. The dependence of surface roughness on the energy per constituent atom reveals that there is an optimum energy for most efficient surface smoothing. Substrate damage increases with dose and cluster energy. For the same dose and *total* cluster energy, larger clusters induce lower substrate damage because multiple collisions are confined to a shallow region closer to the surface.

#### ACKNOWLEDGMENTS

Financial support for this work was provided by the National Science Foundation (CTS-9713262) and the State of Texas through the Texas Advanced technology Program.

- <sup>1</sup> *Handbook of Plasma Processing Technology*, edited by S. M. Rossnagel, J. J. Cuomo, and W. D. Westwood (Noyes, Park Ridge, NJ, 1990).
- <sup>2</sup> T. Seki, T. Kaneko, D. Takeuchi, T. Aoki, J. Matsuo, Z. Insepov, and I. Yamada, Nucl. Instrum. Methods Phys. Res. B **121**, 498 (1997).
- <sup>3</sup> D. J. Vitkavage, C. J. Dale, W. K. Chu, T. G. Finstad, and T. M. Mayer, Nucl. Instrum. Methods Phys. Res. B **13**, 313 (1986); R. J. Davis, A. Climent, and S. J. Fonash, *ibid.* **7/8**, 831 (1985).
- <sup>4</sup> M. Akizuki, J. Matsuo, M. Harada, S. Ogasawara, A. Doi, K. Yoneda, T. Yamaguchi, G. H. Takaoka, C. E. Ascheron, and I. Yamada, Nucl. Instrum. Methods Phys. Res. B **99**, 229 (1995).
- <sup>5</sup> T. Yamaguchi, J. Matsuo, M. Akizuki, C. E. Ascheron, G. H. Takaoka, and I. Yamada, Nucl. Instrum. Methods Phys. Res. B **99**, 237 (1995).
- <sup>6</sup> I. Yamada, J. Matsuo, Z. Insepov, and M. Akizuki, Nucl. Instrum. Methods Phys. Res. B **106**, 165 (1995).
- <sup>7</sup> Z. Insepov and I. Yamada, Nucl. Instrum. Methods Phys. Res. B **121**, 44 (1997).
- <sup>8</sup> J. Matsuo, N. Toyoda, M. Akizuki, and I. Yamada, Nucl. Instrum. Methods Phys. Res. B **121**, 459 (1997).
- <sup>9</sup> P. Sigmund, Phys. Rev. **184**, 383 (1969).
- <sup>10</sup> I. Yamada and G. H. Takaoka, Jpn. J. Appl. Phys., Part 1 **32**, 2121 (1993).
- <sup>11</sup> J. A. Northby, T. Jiang, G. H. Takaoka, I. Yamada, W. L. Brown, and M. Sosnowski, Nucl. Instrum. Methods Phys. Res. B **74**, 336 (1993).
- <sup>12</sup> Z. Insepov, I. Yamada, and M. Sosnowski, J. Vac. Sci. Technol. A **15**, 981 (1997).
- <sup>13</sup> F. H. Stillinger and T. A. Weber, Phys. Rev. B **31**, 5262 (1985).
- <sup>14</sup> L. Marques, M. Caturia, T. D. de la Rubia, and G. H. Gilmer, J. Appl. Phys. **80**, 6160 (1996).
- <sup>15</sup> N. A. Kubota, D. J. Economou, and S. J. Plimpton, J. Appl. Phys. **83**, 4055 (1998).
- <sup>16</sup> A. Rytkonen, S. Valkealathi, and M. Manninen, J. Chem. Phys. **106**, 1888 (1997).
- <sup>17</sup> D. J. Wales and R. S. Berry, J. Chem. Phys. **92**, 4283 (1990).
- <sup>18</sup> L. Ming, N. Markovic, M. Svanberg, and J. B. C. Pettersson, J. Phys. Chem. A **101**, 4011 (1997).
- <sup>19</sup> H. J. C. Berendsen, J. P. M. Postma, W. F. van Gunsteren, A. DiNola, and J. R. Haak, J. Chem. Phys. **81**, 3684 (1984).
- <sup>20</sup> W. C. Swope, H. C. Andersen, P. H. Berens, and K. R. Wilson, J. Chem. Phys. **76**, 637 (1982).
- <sup>21</sup> D. G. Henshaw, Phys. Rev. **111**, 1470 (1958).
- <sup>22</sup> Z. Insepov and I. Yamada, Nucl. Instrum. Methods Phys. Res. B **112**, 16 (1996).